IOSR Journal of Applied Chemistry (IOSR-JAC)
e-ISSN: 2278-5736.Volume 16, Issue 4 Ser. I (April 2023), PP 23-36
www.iosrjournals.org

Formulation and characterization of floor tile composite derived from Polyethylene Terephthalate waste and sand

Emmanuel Mache[1], Dr. Esther Nthiga[2], Prof. Gerald Muthakia[3]

[1]*Chemistry Department, Dedan Kimathi University of Technology, Kenya*

[2]*Chemistry Department, Dedan Kimathi University of Technology, Kenya*

[3]*Chemistry Department, Dedan Kimathi University of Technology, Kenya*

Abstract

In Kenya, the cost of ceramic floor tiles has been increasing due to rapid population growth and urbanization. As a result, there has been significant research into developing affordable composite tiles made from plastics and sand to address this issue. Plastics, particularly PET, causes environmental pollution because they are non-biodegradable and versatile. This study created a stain-resistant and flame-retardant floor tile composite using sand and PET plastic bottle waste as a binder to address this issue. The sand was collected from Ndondo, Isiolo County, while the PET plastic bottle waste was collected from the Nyeri County dump site in Kenya. The composite tile was formulated by varying the amount of sand and keeping the weight of PET plastic bottle waste constant. ZnO was added to the mixture, then coated using a pigment containing TiO_2. The physiochemical properties of the composite tile were assessed according to ASTM standards. The sand used in the study was composed of 93.90% SiO_2, and the composite tile produced with 55.56% sand content had the optimum values for compression strength and tensile strength, and water absorption (104.17 N/mm^2, 12.22 N/mm^2, and 0.21%, respectively). Flame retardation ability improved with adding ZnO, while chemical resistivity depended on the amount of sand added. The composite tile was mainly made of SiO_2 (81.39%) and showed good resistance to acids, bases, swimming pool salts, and household chemicals. The floor tile had varying levels of viscoelasticity (flexible to brittle), depending on the storage modulus. Characterization of the composite revealed that PET and sand had good crosslinking, as evidenced by FTIR analysis. XRF characterization showed that the composite tile was mainly composed of SiO_2 (81.39%). In summary, PET waste bottles can be used as a sand binder to create floor tile composites that are stain-resistant, flame-retardant, and suitable for residential and commercial use.

Keywords: Composite tile, PET, characterization, formulation, waste, cross-linking, flame retardation and viscoelasticity.

Date of Submission: 26-03-2023 Date of Acceptance: 08-04-2023

I. Introduction

The cost of building and construction materials for both commercial and residential properties in Kenya has been rising steadily since 2010, due to a lack of local manufacturing industries that use readily available resources such as sand and clay [1]. A study in 2021 showed that there was a 56% increase in construction material costs in Kenya primarily as a result of rapid population growth, industrialization, and urbanization [2]. Meanwhile, global solid waste production, particularly of plastics, has surpassed 17 billion tons per year, with a projected increase to 27 billion tons by 2050 [3]. This surge in plastic waste production poses significant risks to animals,

humans, and the environment, as highlighted and is a pressing concern for governments, municipalities, and individuals alike [4].

Back in the 1800s, the construction industry mainly used traditional building materials like stone, ceramic, cement, and wood for flooring. But as the 1900s rolled in, new materials like composites came into play. One of the earliest composite flooring materials, linoleum, came about by blending solidified linseed oil, pine resin, ground cork dust, sawdust, and mineral fillers [5]. It was lightweight, corrosion-resistant, and rot-resistant, making it a popular choice in construction. Composite materials, particularly Fiber Reinforced Polymer (FRP) composites, have become increasingly popular in the building industry due to their advantages over traditional materials. FRP composites combine plastic polymer resin with solid fibers, resulting in a strong and consolidated material where each component retains its original shape [6].

In recent years, there has been a growing recognition and acceptance of the importance of green chemistry and technology to promote environmental sustainability, particularly in developing composites. The conventional view of garbage as pollution is gradually being replaced by a new perspective that regards waste as a valuable resource that can aid in achieving sustainable development [7]. Consequently, extensive research has been conducted on recycling solid waste materials, including plastics, into construction materials such as composites, aiming to lower waste volume, construction costs, and demand for natural resources in the construction industry. Plastics, in particular, are of great interest in this sector due to the toxic substances incorporated during their production and gradually released into landfills. African countries like Kenya are particularly affected by plastic pollution due to the high percentage of mismanaged plastic waste and a lack of sophisticated plastic recycling facilities [8].

Previous studies examining the physio-chemical properties of floor tile composites produced from plastic waste have demonstrated that such composites possess strong mechanical features, high water resistivity, and fire. One such study analyzed floor tile composites made from PET and PE waste plastics and discovered that these composites possess a density of 1.44 g/cm^3, compressive strength of 15.5 MPa, and water absorption of 0.3%. The study also determined that the composites are fire and insect-resistant. Another study examined the characteristics of floor tile composites produced from waste PP and HDPE plastics and found that the composites have a density of 1.2 g/cm^3, compressive strength of 35 MPa, and water absorption of 0.2%. Therefore, more research is necessary to evaluate the long-term performance of these composites in real-world applications despite their promising properties [9].

The traditional method of producing floor tiles typically involves using clay and quartz sand, but this study explored alternative economically feasible methods for making composite tiles [10]. The study used a combination of silica sand containing quartz (SiO_2 and SiO_4), PET plastic bottle waste, and ZnO to develop a composite floor tile resistant to stains and it's a flame retardant tile. The physical and chemical properties of the composite tile, such as compression strength, tensile strength, stain resistance, flame retardation, viscoelasticity, and chemical resistance, were tested to determine if it could replace commercial ceramic tiles. XRF was used to characterize the elemental composition of the sand and composite tile, while FTIR was used to evaluate the binding capacity of PET to sand.

II. Methodology

PET Plastic Waste bottles Collection

The PET plastic bottle waste samples were collected from the Nyeri County dumping site, while sand samples were collected from the Ndondo area in Isiolo County, Kenya.

Elemental Composition Analysis of Sand

The sand samples were randomly collected from the Ndondo area in Isiolo County, Kenya. They were sun-dried before being sieved to a consistent grain size of 2 mm. The sand samples used in this study were characterized using XRF S1 TITAN model number 500S with an SDD silicon drift detector having a resolution of 145 eV. The elemental analysis methods were adopted from studies conducted by [11] [12].

Floor Tile Composite Formulation

In this study, techniques from [13] [14] were utilized to formulate the composite floor tiles using PET plastic bottles, ZnO, and sand. To prepare the materials, the PET bottles were cleaned and dried in the sun, then cut into tiny pieces, and the sand was also sun-dried and sieved to achieve 2mm grain sizes. The weight of the PET plastic

waste (200g) while the amount of sand varied between 100g, 150g, 200g, 250g, 300g, 350g, and 400g in the composite formulation. Metal molds were used to shape the composite tiles, which were dried and cured for 24 hours before being characterized.

Physical Tests

Compressive Strength Test

The compressive strength of the formulated composite floor tiles was tested using the DDHCTM model number STYE-2000 and ASTM C1424 standards. Samples with dimensions of 100mm x 100mm x 100mm were prepared and placed in a UTM, where a load was applied until the sample broke, and the maximum load applied was recorded. Equation (1) was used to calculate the compression strength.

$$\text{Compression Strength} = \frac{Force\ Applied}{Area} \quad (1)$$

Tensile strength

The tensile strength of the floor tile composites was tested in accordance with ISO 10545 standards using a Universal Testing Machine (UTM) of model WA-100B [15]. Equation (2) was used to calculate the compression strength.

$$\text{Tensile Strength} = \frac{Force\ Applied}{Area} \quad (2)$$

Viscoelasticity (Storage modulus)

The storage modulus of composite floor tiles was examined per the ASTM C627 standards using a WA-100B UTM. The composite samples were shaped into cubes that measured 100mm on each side. The samples were subjected to a consistent force to determine their storage modulus. In contrast, the displacement of the sample was monitored with a displacement transducer, and the force applied to the sample was measured using a load cell connected to the UTM. The storage modulus of the samples was calculated using equation (3) and then compared with any changes detected in the tensile strength of the composite floor tile.

$$\text{Storage Modulus (G')} = \frac{Stress}{Strain} \quad (3)$$

Where, Stress = Force / Area and Strain = Deformation / Original Length

Water Absorption Test (WA)

The ability of composite floor tiles to absorb water was evaluated according to the ASTM C373-88 guidelines. To do this, samples of the tiles were prepared in 100 mm x 100 mm x 10 0mm sizes, weighed (M1), and submerged in 250 mL of distilled water for a week. After letting them drip for 30 mins, the samples were weighed again (M2). The water absorption of each tile was determined using Equation (4).

$$Water\ Absorption = \frac{M2-M1}{M1} \times 100\% \quad (4)$$

Where M1 is the original weight of the ceramic material and M2 is the final weigh of the composite material after immersion in water.

Chemical Resistance Tests

The ISO 10545-13 standards were followed to test how well the composite tiles could withstand exposure to different chemicals. The composite tile samples for this study were cut into 50mm x 50mm x 50mm pieces, which were weighed (W1). For seven days, these samples were soaked in various chemicals, including household chemicals, swimming pool salt, strong and weak acids, and alkalis. After the soaking period, the samples were taken out of the water and left to drip for 30 minutes before being weighed again (W2). To determine the Chemical of each composite tile sample, equation (4) was used.

$$Chemical\ Resistivity = \frac{W2-W1}{W1} \times 100\% \quad (5)$$

The chemicals used in this test were prepared as shown;

Household chemical

The common household chemical used in this study was Ammonium chloride (NH_4Cl) solution, 100 g/l.

Swimming pool salt

Sodium hypochlorite (NaClO) solution of 20 mg/l prepared from technical grade sodium hypochlorite solution 5% (W/V) was used for this test.

Acids and alkalis

Low concentrations

The acid used in this test was 3% hydrochloric acid solution. This acid was prepared from 40% v/v concentrated HCl. Moreover, 30g/L KOH was used as an alkali in this test.

High concentrations

For the high concentration in the acids and alkali tests, an 18% hydrochloric acid solution prepared from 40% v/v concentrated H_2SO_4 was used. In addition, 100g/L KOH was used as an alkali in this test.

Flame Retardation Test

The flame retardation ability test in this study aimed to assess the flame retardation ability of a composite tile with the optimum physio-chemical properties (Composite D with the ratio of sand to PET of 5:4) by varying the amount of ZnO in the composite from 0 g to 30 g. The ASTM D635 standard was used to determine the linear burning rates of 7 composite tile samples. The samples were prepared by cutting them into 100 mm bars, applying paraffin to the top end, and igniting them with a Bunsen burner. The time taken for the flame to extinguish was recorded, and the linear burning rate was calculated using equation (6).

$$V = \frac{60L}{T} \quad (6)$$

Where V- Linear burning rate in mm/min, L - Burned length in millimeters and T - Period in minutes.

Stain Resistivity of the floor tile composite

After the physical and chemical resistivity tests were done, the coated and uncoated tiles' stain resistivity were tested using ISO 10545-14 standards. This test was done for the tile that had high chemical resistivity and physical property. Iodine Solution and Rhodamine B Dye are the two dyes used in this test. Iodine solution was prepared by mixing a 2% potassium iodide solution in water. Rhodamine B Dye. Rhodamine B dye was prepared by mixing water, ethanol, and glacial acetic acid in a ratio of 70:30:1 [16] [17].

III. Results and Discussions

Characterization using XRF

4.1.1 Elemental analysis of sand

The elemental composition of the sand used in the formulation of the floor tile composite was determined by XRF spectroscopy. Table 1 shows the elemental composition of the sand sample used in this study.

Table 1: The elemental composition of the sand used in the composite formulation

Constituent	SiO_2	Al_2O_3	MgO	P_2O_5	S	Fe	K_2O	CaO	TiO_2	Sr	Zr	Ba
Composition Percentage (%)	93.9	0.97	0.87	0.12	0.04	2.42	0.37	0.6	0.45	0.19	0.06	0.14

According to Table 1, the sand analyzed in this study consisted mainly of SiO_2, which classified it as silica sand with a content of 93.90%. Iron was also found in the sand sample at a concentration of 2.42%, a common impurity affecting sand properties depending on its concentration. However, since the iron content in this sand sample was low, it did not significantly affect its suitability for construction applications Additionally, the sand maintained its natural white color as a result of the high SiO_2 content [18]. Other impurities in the sand, including Al_2O_3, MgO, Ti, and S, were also present in low concentrations, with compositions of 0.97%, 0.87%, 0.45%, and 0.04%, respectively. These impurities are known to affect sand properties. Since the concentrations of these impurities were below 5% of the total weight in the sand sample used in this study, their impact on the floor tile composite's properties was insignificant. XRF analysis confirmed that the sand used in the floor tile composite had high SiO_2 and low impurity concentrations, making it suitable for building and construction applications [19].

Elemental analysis of the Floor Tile Composite

XRF spectroscopy was utilized in the inorganic elemental composition characterization of the formulated floor tile composite.

Table 2:Inorganic Elemental Composition of the Floor Tile Composite.

Constituent	SiO_2	Al_2O_3	MgO	P_2O_5	S	Fe	K_2O	CaO	TiO_2	Zn	Sr	Zr	Ba
Composition (%)	81.39	1.88	0.21	0.02	0.31	7.16	2.77	3.35	2.41	0.15	0.12	0.08	0.17

According to Table 2, the composite floor tile had the highest SiO_2 composition at 81.39%. However, this was still lower than the original SiO_2 content in the sand used. This difference is due to the use of quartz during crosslinking and bond formation of Si-O-Si and Si-O-C bonds[20 21]. The amount of Al_2O_3 in the composite increased to 1.88% due to the PET plastic bottle waste used in the formulation, which contains Al_2O_3 as a coating material. This coating material enhances barrier properties, making it more resistant to gas and moisture permeation. The composite's stain resistivity property, provided by TiO_2, also increased to 2.41%. This is because both the sand and PET used in the formulation contained TiO_2, which acts as a UV stabilizer in PET[22].

Characterization using FTIR

FTIR spectra of raw Sand

In this study, sand was analyzed using FTIR analysis to characterize it. This characterization aimed to detect the existence of different chemical functional groups and recognize particular minerals, impurities, or other chemical substances found in the sand utilized for the floor tile formulation.

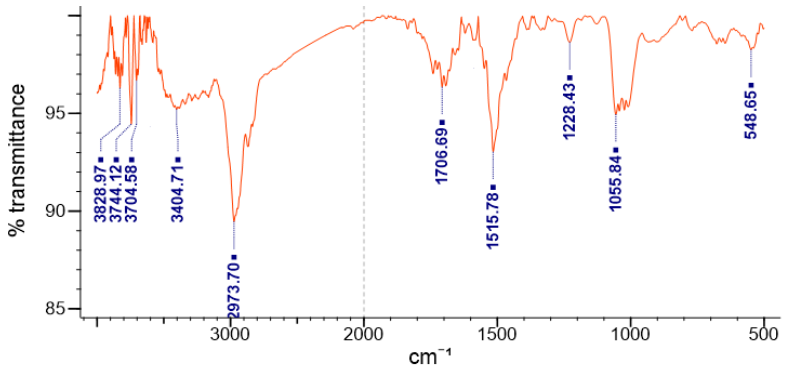

Figure 1:FTIR Spectrum of the sand used in the floor tile composite formulation

The FTIR Spectrum of the sand used in the floor tile composite formulation (Figure 1) revealed the stretching of TiO2 bonds in the 750-550 cm^{-1} region, confirming the presence of TiO_2 in the sand sample [23]. The stretching vibrations of Al-O bonds were also observed in the range of 1400 – 1260 cm^{-1}, indicating the presence of aluminum compounds, which are feldspar or clay. Additionally, the 3100–2800 cm^{-1} region was associated

with aromatic and aliphatic –C–H symmetrical stretching, possibly indicating the presence of organic compounds or hydrocarbons in the sand [24]. The region between 3600-3200 cm^{-1} was associated with stretching OH bonds, suggesting the presence of hydroxyl, which is present in minerals such as mica or clay, common components of sand. The stretching vibrations of Si-O-Si and SiO_4 bonds were observed in the 1200 – 1000 cm-1 region, confirming the presence of SiO_2 in the sand sample. The bending of -Si-O-Si bonds observed at peak 548 cm^{-1} also indicates the presence of SiO_2 [25]. The FTIR analysis suggests that the sand sample used in this study mainly comprises SiO_2 (quartz) with aluminum and titanium compounds impurities. OH, bonds suggest the presence of water or moisture in the sample.

FTIR spectrum for Composite tile

The functional groups in the composite tile were identified using FTIR to demonstrate the cross-linking and bonding between PET and SiO_2 during the formulation process, resulting in the formation of the composite.

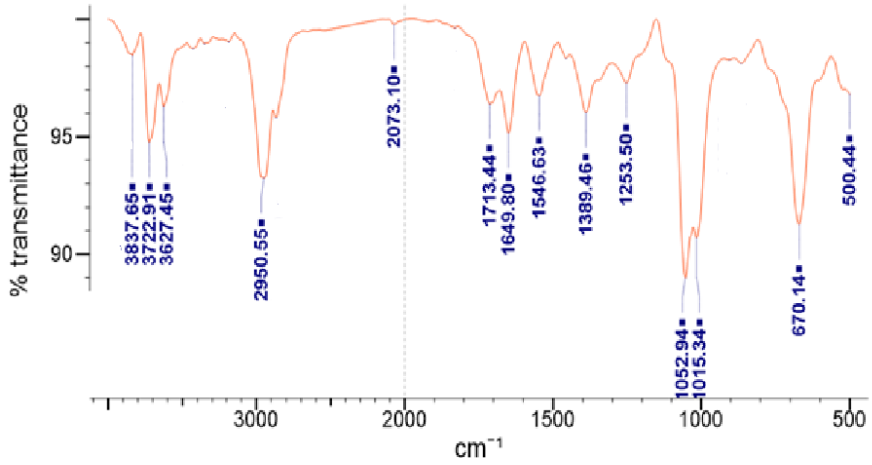

Figure 2: Composite tile's FTIR spectrum

From the FTIR spectrum (Figure 2) of the composite tile, the stretching of TiO_2 bonds is observed in the region between 750-600 cm^{-1}, which indicates the presence of TiO_2 in the composite tile [26]. The TiO_2 is from the sand used during the formulation of the composite tile. The Si—H group is readily identified by a strong band in the range 2280-2070 cm^{-1}, indicating the presence of silanes in the composite tile [27]. Silanes are commonly used as coupling agents to improve the composites' adhesion between the filler and the matrix. Furthermore, the FTIR spectrum shows a band at about 1200 -1000 cm^{-1}, attributed to the Si-O-Si and Si-O-C bonds typically observed in alkoxysilanes which also acted as a coupling agent in the tile composite during crosslinking [25]. In summary, the FTIR spectrum of the composite tile provided detailed information about the functional groups present in the tile, including TiO_2, silica, silanes groups which showed the presence of crosslinking between SiO_2 in sand and PET.

Physical Properties of the composite tile

Water Absorption Ability (WA)

The capacity of the floor tile composite to absorb water was measured by calculating the percentage difference in weight.

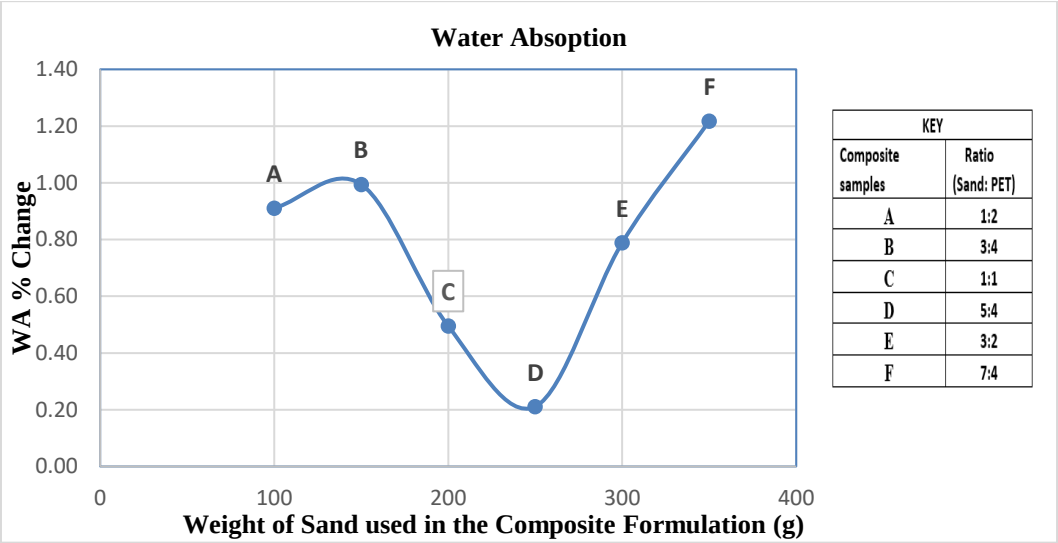

Figure 3:A graph of how water absorption ability (WA) is affected with the amount of sand in the composite (PET, 200g constant).

Figure 3 shows how WA of the composite is affected with the amount of sand added during the formulation of the composite tile. From figure 3 results, the WA values of the six tile composite samples tested ranged from 0.21% to 1.22%. Water absorption ability decreased with increase in amount of sand to 0.21% (300 g of sand), beyond that the increase in amount of sand increased the WA. Decrease in WA at low sand level was attributed to the crosslinking between sand and PET increased . However, the WA values were seen to increase beyond ratios of D (5:4) which can be explained by the fact that as sand content increased, there was reduction in crosslinking and binding between sand and PET which increases the composite's porosity [28]. The formulated composite had a water absorption rate of 0.2% lower than the previous studies of similar materials [29]. This difference can be caused by geographical source of sand and the type of plastic used among other factors. In conclusion, according to ASTM C373-88 standards, tiles A (1:2), B (3:4), and C (1:1) are classified vitreous, which means they are suitable for indoor use [30]. However, tile composites D (5:4) and E (3:2) are classified as impervious tiles, making them appropriate for both indoor and outdoor applications hence can be used as floor tiles [31].

Compressive Strength Test

The compressive strength of composite tiles that were created was evaluated using samples containing different ratios of sand to PET of 1:2, 3:4, 1:1, 5:4, 3:2, and 7:4.

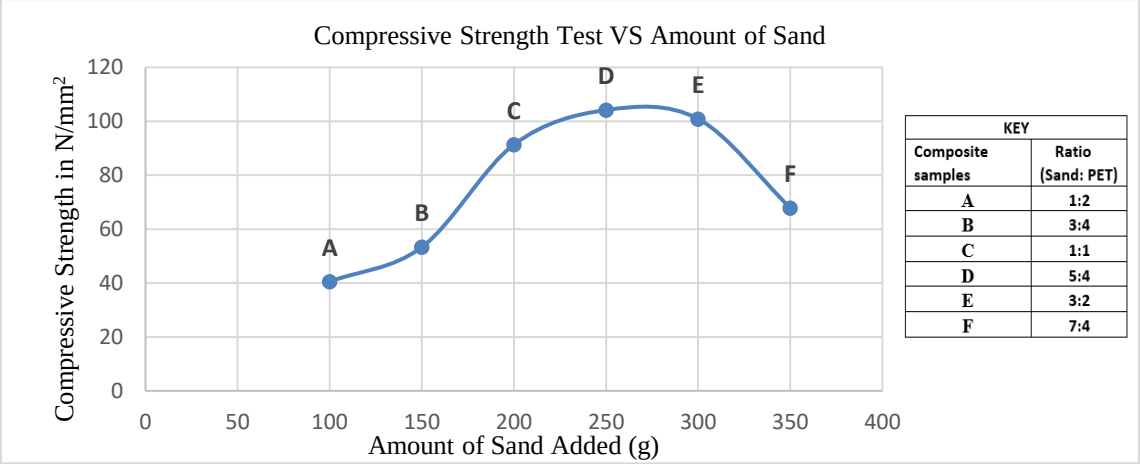

Figure 4:A graph showing how Compressive strength of the composite changes with the amount of sand (PET, 200g constant).

According to Figure 4, which displays the relationship between the Compressive strength of the composite and the amount of sand, it is evident that the compression strength of the composite increased as the amount of sand in the mixture was increased. The optimum compression strength of the composite was observed to be 104.17 N/mm^2 for the 5:4 (D) composite. The reason for the increase in compression strength is believed to be due to the enhanced ability of PET to crosslink with silica, resulting in an improved filler/matrix ratio for the composite [32]. Compression strength decreased between samples 3:2 to 7:4 due to reduced filler/matrix ratio composite. This was caused by weaker binding between the sand and PET resulting from adding more sand while keeping the amount of PET constant. These values were greater than the values reported by [33] because this study only involved varying sand ratios. Additionally, this study reported a compressive strength of 5.1 N/mm^2 for studies done on mechanical properties of plastic sand brick containing plastic waste [33]. From the results, the formed composite floor tiles' total strength is impacted by the filler/matrix ratio of PET and sand [34]. Additionally, the overall compressive strength of the tile composite is impacted by the PET's capacity to bind to silica sand [35]. The compressive strength values had a p-value of 0.003 which was statistically significant at $p \leq 0.05$ level. Moreover, the formulated composite tiles meet the standards set by ASTM C648 which sets the minimum compression strength at 13.8 N/mm² for composite tiles [36].

Relationship of Viscoelasticity (Storage modulus) and Tensile strength

This test aimed to investigate the impact of altering the quantity of sand in the composite substance on its viscoelastic characteristics. The study compared the material's capacity to endure stretching forces without fracturing to the storage modulus.

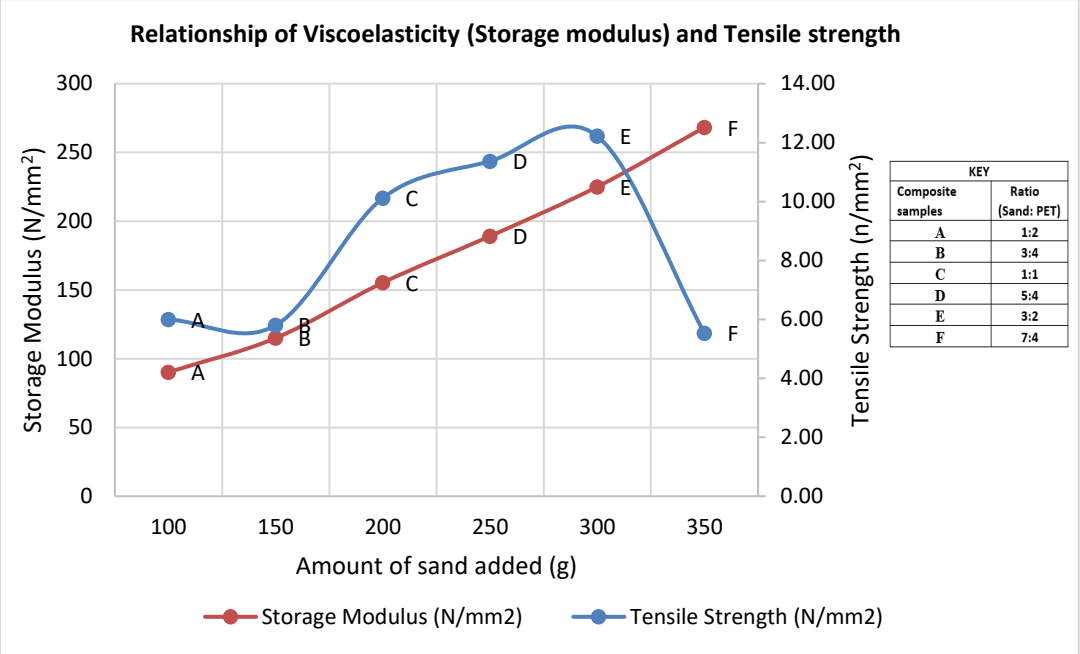

Figure 5: A graph the relationship between viscoelasticity (Storage Modulus) and Tensile strength

The results in figure 5 indicate that the composite material's tensile strength improved as the amount of sand added increased until it reached 300 g. At this point, the highest tensile strength of 12.22 N/mm^2 was achieved, followed by a decline in strength to 5.53 N/mm^2 at 350 g of sand wight. In addition, the storage modulus also rose with increasing sand content, beginning at 90.22 N/mm^2 with 100 g sand content and steadily rising to 268.22 N/mm^2 with 350 g sand content. This behavior implies that adding sand increases the composite material's rigidity and tensile strength [37]. The rise in tensile strength and storage modulus can be credited to the PET and sand being cross-linked. A higher amount of sand increases the cross-linking between the polymer chains, resulting in greater rigidity and strength. Nevertheless, when the sand content reaches 350 g, there is a significant reduction in tensile strength. This may be due to an excessive amount of sand, which could have led to a decrease in cross-linking density and weaker bonding between the PET polymer matrix and sand particles. As a result, the composite material became weaker. Introducing sand into the composite floor tiles increased the tensile strength and storage modulus. The improvement in these properties is due to the cross-linking of the polymer chains. However, when sand content is in excess, the tensile strength reduces due to the weakening of the cross-linking and adhesion between PET and sand [38].

In conclusion, the storage modulus values increased with increasing sand content, indicating increased stiffness and ability to store elastic energy. On the other hand, the decrease in tensile strength with excess sand content suggests that the composite material also exhibits viscous behavior. Therefore, the composite material studied can be classified as viscoelastic, exhibiting both elastic and viscous behaviors depending on the sand content.

Flame Retardation Test

The composite tile's resistance to flames was evaluated by varying the quantity of ZnO added to the tile. Additionally, this experiment aimed to determine if the ZnO addition could serve as a flame retardant.

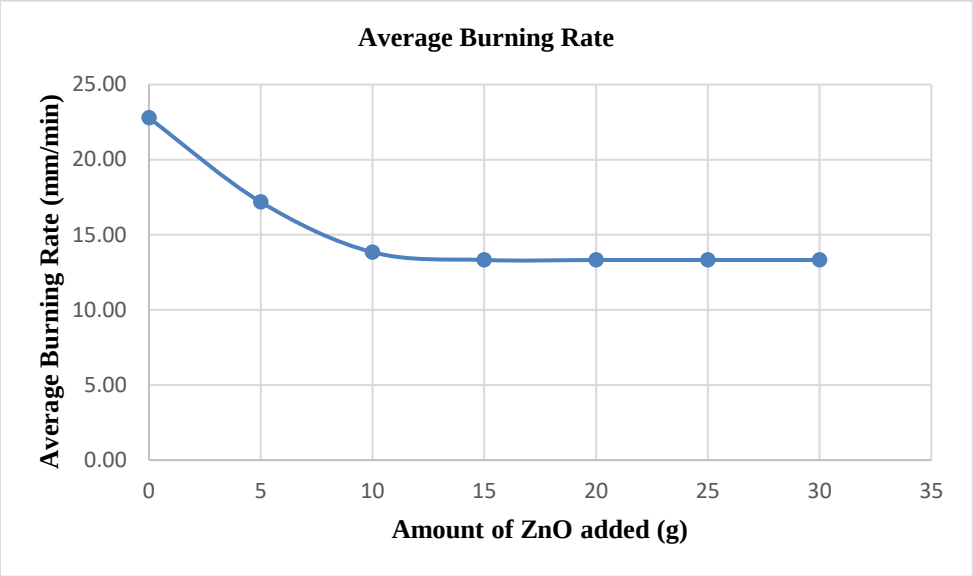

Figure 6: A graph of Linear Burning Rate (mm/min) of the composite samples.

According to Figure 6, the composite samples' linear burning rate (measured in mm/min) decreased as the amount of added ZnO increased. However, the burning rate reached its best level when 15 g of ZnO was added, with a burning rate of 13.32 mm/min. ZnO contributes to flame retardancy in two ways: through thermal and gas-phase mechanisms. In the thermal mechanism, ZnO absorbs heat generated during combustion and decomposes, releasing oxygen. This oxygen reacts with free radicals and volatile gases produced during combustion, suppressing the combustion process as demonstrated in equation 7.

$$ZnO \longrightarrow Zn + 1/2\ O_2 \quad (7)$$

The gas-phase mechanism involves the reaction of ZnO with the volatile gases generated during combustion to create solid and stable zinc compounds. This eliminates the fuel source for the combustion process and prevents the fire from spreading. Moreover, the combustion rate decreases because the sand's SiO_2 and Al_2O_3 have already undergone complete oxidation, making them unable to burn further. This limits the carbonization of polymers and leads to heat absorption, which creates a barrier to suffocate the fire and reduce the oxygen supply. This ultimately lowers the combustion rate [39]. The minimum linear burning rate of the formulated floor tile composite was between 13.32 mm/min which are much lower than published values of similar work by [40] [14]. The values in this study were lower because the ZnO used in the formulation of this tile increased char formation, inhibiting flame spread even further [41]. Incorporating ZnO into the composite tile matrix has decreased the tile's linear burning rate, suggesting that it functions as a flame retardant. This effect is probably due to thermal and gas-phase processes, whereby ZnO absorbs heat, emits oxygen, and interacts with unstable gases to form stable compounds, which restrict the propagation of the flame. The tile specimens satisfy the requirements for being classified as flame retardant tile, as per NFPA 101 standards, since their burning rate is no less than 38mm/min.

Chemical Resistivity Tests

Household chemicals

The sand-PET composite tiles with ratios of 1:2, 3:4, 1:1, 5:4, 3:2, and 7:4 was subjected to a resistivity test against NH_4Cl for seven days.

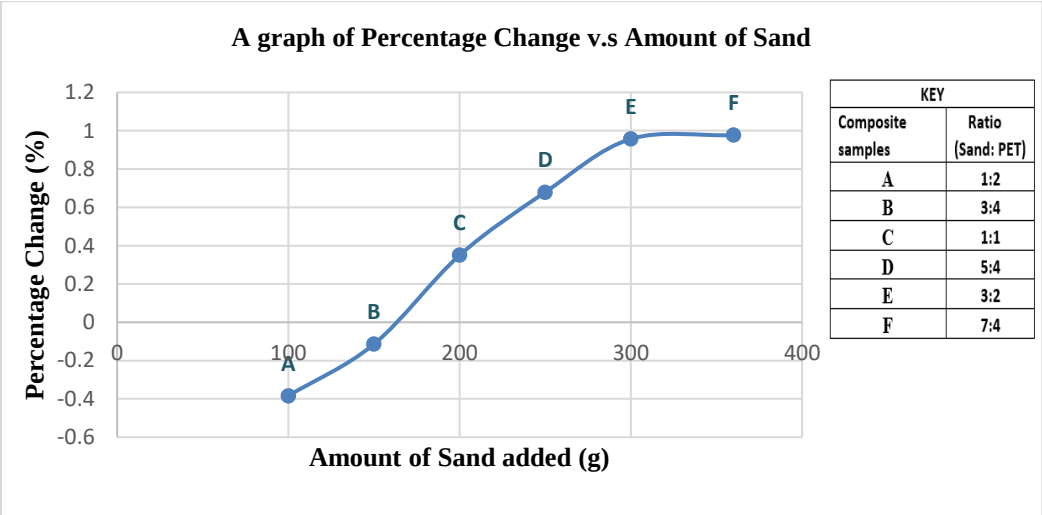

Figure 7: A graph of percentage change versus amount of sand when emerced in 100g/L NH_4Cl

The graph presented in Figure 7 displays the correlation between the percentage change and the quantity of sand when immersed in NH_4Cl solution with a concentration of 100 g/L. Based on the graph, an increase in sand resulted in a reduced mass loss in the composites. This indicates that the composite's resistance to NH4Cl increased as the sand content increased. The mass loss in composites with lower sand compositions is because ammonium salts are typically more reactive than other types of base salts[42]. The primary way the NH_4Cl solution interacts with metal oxides (such as SiO2) is by creating metal complexes with chloride and ammine. This chemical reaction between NH_4Cl and SiO_2 is classified as an acid-base reaction since ammonium chloride is an acidic salt and silicon dioxide is a basic oxide. Equation 7 displays the chemical reaction.

$$NH_4Cl + SiO_2 \longrightarrow NH_3 + H_2O + SiCl_4 \quad (8)$$

The chemical process involves the combination of ammonium chloride and silicon dioxide, which results in the creation of ammonia (NH_3), water (H_2O), and silicon tetrachloride ($SiCl_4$). To summarize, ammonium chloride and silicon dioxide reaction produce ammonia, water, and silicon tetrachloride [43]. Composite 7:4 displayed the greatest resistance to NH_4Cl (0.98%) compared to composite 1:2, which showed the lowest resistivity (-0.38%). The average resistivity was 0.41%, and the p-value was 0.16.The figures of this study are lower than the values reported by [44] because the incorporation of more organic additives (PET) in this study as opposed to cement increased resistivity of this composite toward NH_4Cl [44]. According to EN 14411 standards the maximum weight loss allowed for a tile for chemical resistivity is set at 1%. Since the average resistivity of the tile is 0.41%, the tile is resistant to NH_4Cl and is classified as class 1 tile.

Swimming pool salts

The formulated composite tiles of sand to PET ratios of 1:2, 3:4, 1:1, 5:4, 3:2, and 7:4 was tested for their resistivity against NaClO for a period of 7 days.

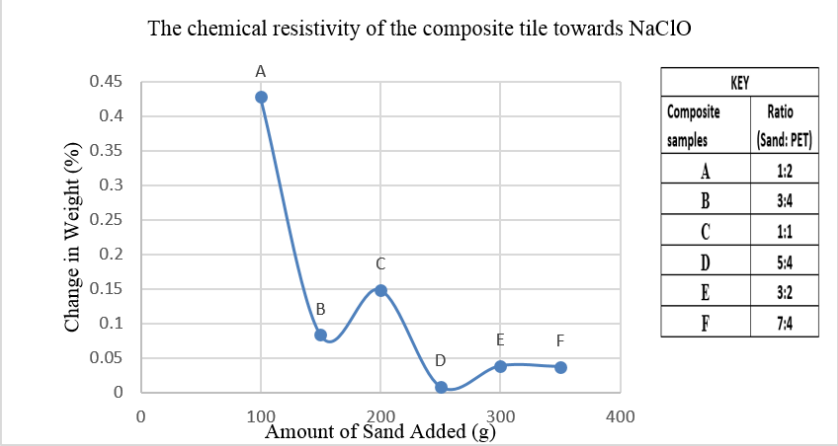

Figure 8: The chemical resistivity of the composite tile towards NaClO by varying the amount of sand and the amount of PET constant at 200 g.

The findings depicted in figure 8 indicate that as the quantity of sand increased to 250g, there was a reduction in the percentage change in the weight of the composite tile. After that, the percentage change in weight slightly increased for larger quantities of sand. This implies that the composite tile containing 250g of sand demonstrated superior chemical resistivity towards NaClO (0.009%). This is because SiO_2 has high chemical resistivity towards NaClO, and the increased concentration of SiO_2 resulting from the increased amount of sand in the composite tile enhances chemical resistivity. Nevertheless, when the sand quantity gets excessively high, the mechanical attributes of the composite tile may be undermined because of the reaction between NaClO and the extra SiO2, causing a slight reduction in chemical resistivity [45]. The chemical reaction that occurs between SiO_2 and NaClO is shown as follows:

$$SiO_2 + 2NaOCl \rightarrow Na_2SiO_3 + 2NaCl + O_2 \quad (9)$$

These results indicate that increasing the amount of sand in the composite tile up to a specific limit can increase its chemical resistivity towards NaClO [46]. Moreover, at very high amounts, the mechanical properties of the composite tile may be compromised. These figures demonstrate that the formulated floor tile composites are resistant to swimming pool salts i.e. NaClO and can be classified as GA tiles since the resistivity of the tile shows that weight loss for all the samples is below 1% [47].

Acids and Alkalis

Resistivity to low and high concentration hydrochloric acid solution

The resistance of composite tiles made from different ratios of sand to PET i.e., 1:2, 3:4, 1:1, 5:4, 3:2, and 7:4 against HCl was tested.

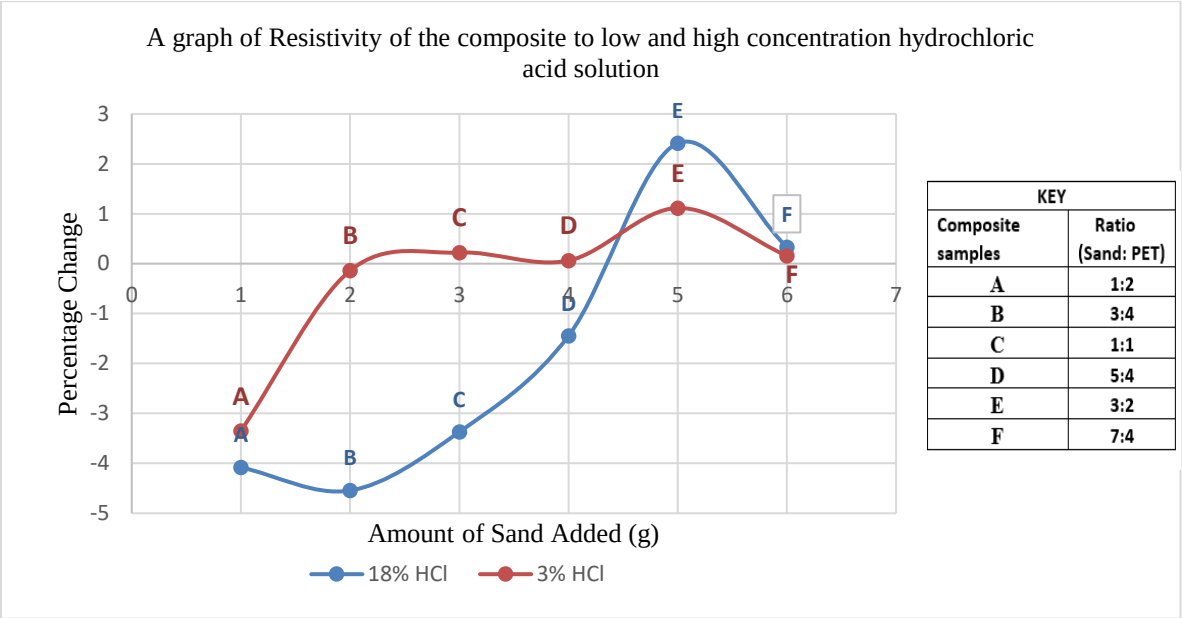

Figure 9:A graph of Resistivity of the composite to low and high concentration hydrochloric acid solution

The resistance of the tile composite formulated against 18% HCl and 3% HCl, investigated as per ISO 10545-13 standards, is illustrated in Figure 18. The results indicate that the tile composites became more resistant to HCl corrosion with increased sand content, and minimal weight loss. The composite showed the highest resistance to both high and low concentrations of HCl at a sand content of 300g (E), with resistivity values of 2.411% and 1.115%, respectively. The improved ability of composites to resist HCl is due to the presence of PET, which prevent aggressive solutions from passing through and decrease the absorption of any corrosion causing solvent into PET-mortar composites [44] [48]. Furthermore, PET is resistant to HCl because of its unique chemical structure. The presence of ester groups in PET's molecular structure makes it resistant to acid attack [49]. This is because the ester groups have a resonance structure, which means that electrons can move between the two oxygen atoms in the ester group, making them less susceptible to breaking apart. Additionally, the reduction in porosity in the composite matrix was caused by the incorporation of HCl resistant sand granules which greatly contributed to the reduction HCl solution absorption, hence by minimal weight loss in the composite tile. These findings are consistent with those reported by [44]. It should also be noted that the concentration and nature of the acid have an effect on the chemical resistance of materials. According to the graph (Figure 18), 18% HCl is more corrosive than 3% HCl [50]. Since the average weight loss of the tile is below 1% , these composite tiles are resistant to HCl and is classified as class 1 tile.

Resistivity to low and high concentration potassium hydroxide solution

To evaluate the resistance of composite tiles to strong and weak KOH solutions, samples formulated with varying sand-to-PET ratios (1:2, 3:4, 1:1, 5:4, 3:2, and 7:4) were tested for seven days.

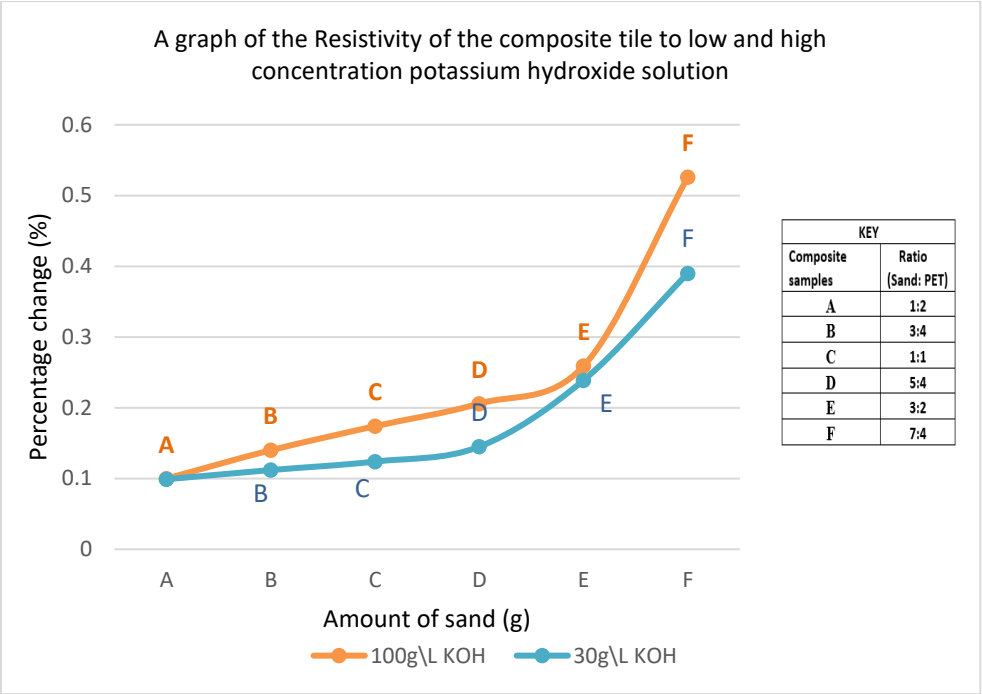

Figure 10:A graph of the Resistivity of the composite tile to low and high concentration potassium hydroxide solution.

Figure 10 illustrates the resistivity of the composite tile to low and high-concentration KOH solution. The graph indicates that as the concentration of sand in the composite material increased, the tile's resistance to KOH decreased. This trend is because KOH does not typically affect most types of plastic, such as PET, despite being a good solvent for dissolving organic substances [51]. In contrast, the sand's SiO_2 reacts with potassium hydroxide to produce potassium metasilicate, water and potassium metatetrasilicate [52]. Both reactions take place as shown in equation 10;

$$4KOH + 2SiO_2 \rightarrow K_2SiO_3 + K_2Si_4O_5 + 2H_2O \quad (10)$$

Sample A containing 100 g of sand, exhibited the strongest resistance to KOH, as indicated by Figure 10, with 0.100% and 0.099% readings for KOH concentrations of 100gL and 30g/L, respectively. These results were lower than those reported by [53] but consistent with the findings of [44]. The consistency in the results is attributed to using similar materials and conditions in the study. Furthermore, the average weight loss of the tile was less than 1%, demonstrating that these composite tiles are resistant to KOH and are classified as class 1 tiles.

Stain Resistance Property

The coated and uncoated tiles were subjected to a test for stain resistivity that followed the ISO 10545-14 standards. Once all the physical and chemical tests were completed, the composite tile with the best properties (Composite D) was split into coated and uncoated. Eight samples were taken from each group and stained with Iodine Solution and Rhodamine B Dye for 24 hours. After cleaning, the samples were classified based on their stain-removal capabilities. Classification 5 indicates that the stain was removed with hot water at 55°C. Class 4 means the stain was removed with a weak cleaning agent (soap) and non-abrasive cloth. Class 3 means the stain was removed with a strong bristle brush and a strong cleaning agent (bleach). Class 2 indicates the stain was removed by soaking the sample in a strong solvent (Acetone) for 24 hours. Class 1 indicates that the stain was not removed.

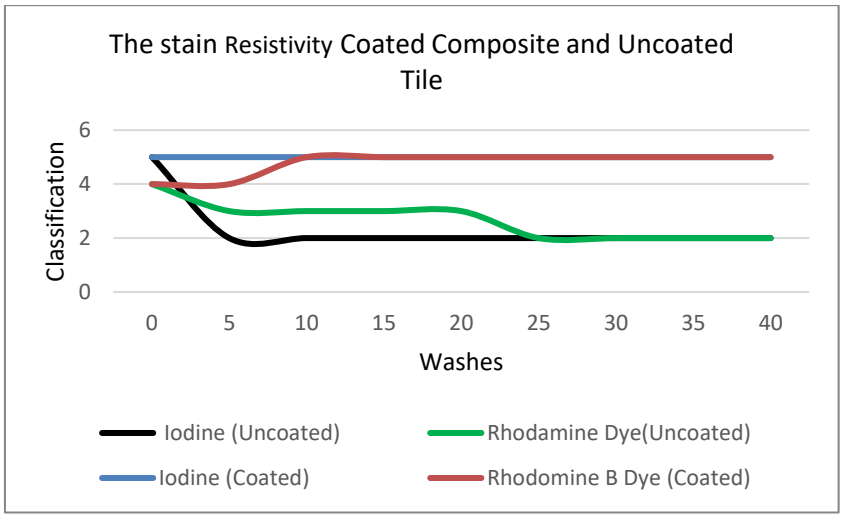

Figure 9:A graph of stain resistivity and classification of the Coated and Uncoated composite tile toward Iodine and Rhodamine B Dye.

Uncoated tile

The uncoated composite tile was analyzed for its ability to resist stains using Iodine and Rhodamine B Dye. The results, shown in Figure 9, indicate that the tile could resist Rhodamine B Dye for up to 20 washes and iodine stains for up to 25 washes. The test results classify the uncoated composite tile as a Class 2 tile, which means it is unsuitable for high-traffic areas like bathrooms, kitchens, and commercial spaces [54].

Coated Tile

Figure 9 illustrates the evaluation of the stain resistance and classification of a composite tile coated with a layer that was tested against Iodine and Rhodamine B Dye. According to the results, the coated tile could resist Rhodamine B Dye for up to 10 washes and iodine stains for up to 10 washes. Consequently, the coated composite tile has been classified as a Class 5 tile. The composite tile outperformed the uncoated tile due to TiO_2, which functions as a stain-resistant layer in the composite. This means the composite tile can withstand the effects of heavily staining substances such as coffee, red wine, and oil-based products [54].

IV. Conclusions

This study's investigation and experimental results show that PET wastes can be used as a binder in the formulation of floor tile composites when combined with natural sand. Moreover, the addition of ZnO in the matrix of the composite helps to improve the composite's flame retardation ability. Coating the composite with a pigment containing TiO_2 helped in enhancing the stain resistivity of the floor tile composite. Moreover, the results from this study show that household chemicals, swimming pool salts, acids, and bases do not affect the floor tile composite formulated from PET wastes, sand, zinc (II) oxide, and titanium (IV) oxide. The floor tile composite from PET wastes, sand, zinc (II) oxide, and titanium (IV) oxide is a flame retardant. These results show that PET and sand can be used to develop floor tile composites that are thermally stable and resistant to chemicals provided by SiO_2 in the sand. At the same time, PET offers a composite with high strength and flexibility, high compression, and tensile strength.

V. Recommendations

The PET plastic waste must be melted and treated using an appropriate machine to create a consistent blend with the sand. However, this process may generate hazardous gases that cannot be easily contained in a gas chamber. Depending on the desired characteristics of the end product, it may be beneficial to include additives like UV stabilizers or colorants. Incorporating these additives can enhance the tiles' resistance to weather and fire and improve their aesthetic appearance.

References

[1]. Tay, Y. W. D.; Panda, B.; Paul, S. C.; Noor Mohamed, N. A.; Tan, M. J.; Leong, K. F. 3D printing trends in building and construction industry: A review. Virtual and Physical Prototyping. **2017**; 12 (3): 261-276.

[2]. Ratcliffe, J.; Stubbs, M.; Keeping, M. Urban planning and real estate development; Routledge: Milton Park , 2021;Volume 8. Pp 15-108

[3]. Karak, T.; Bhagat, R.; Bhattacharyya, P. Municipal solid waste generation, composition, and management: the world scenario. Critical Reviews in Environmental Science and Technology. **2012**; 42 (15): 15-100.

[4]. Yong, C. Q. Y.; Valiyaveettil, S.; Tang, B. L. Toxicity of Microplastics and Nanoplastics in Mammalian Systems. International Journal of Environment and Public Health. **2020**; 17 (5): 1-8. DOI: 10.3390/ijerph17051509.

[5]. Torres-Giner, S.; Montanes, N.; Fenollar, O.; García-Sanoguera, D.; Balart, R. Development and optimization of renewable vinyl plastisol/wood flour composites exposed to ultraviolet radiation. Materials & Design. **2016**; 108: 648-658.

[6]. Sampaio, A. Z.; Pinto, A. M.; Gomes, A. M.; Sanchez-Lite, A. Generation of an HBIM Library regarding a Palace of the 19th Century in Lisbon. Applied Sciences. **2021**; 11 (15): 2-8.

[7]. Tang, Z.; Li, W.; Tam, V. W. Y.; Xue, C. Advanced progress in recycling municipal and construction solid wastes for manufacturing sustainable construction materials. Resources, Conservation & Recycling. **2020**; 6:2-18. DOI: 10.1016/j.rcrx.2020.100036.

[8]. Jambeck, J.; Hardesty, B. D.; Brooks, A. L.; Friend, T.; Teleki, K.; Fabres, J.; Beaudoin, Y.; Bamba, A.; Francis, J.; Ribbink, A. J.; et al. Challenges and emerging solutions to the land-based plastic waste issue in Africa. Marine Policy. **2018**; 96: 256-263. DOI: 10.1016/j.marpol.2017.10.041.

[9]. Almeshal, I.; Tayeh, B. A.; Alyousef, R.; Alabduljabbar, H.; Mohamed, A. M.; Alaskar, A. Use of recycled plastic as fine aggregate in cementitious composites: A review. Journal of Construction and Building Materials. **2020**; 253: 4.

[10]. Moussi, B.; Hajjaji, W.; Hachani, M.; Hatira, N.; Labrincha, J.; Yans, J.; Jamoussi, F. Numidian clay deposits as raw material for ceramics tile manufacturing. Journal of African Earth Sciences. **2020**;164: 2-6.

[11]. Weindorf, D. C.; Bakr, N.; Zhu, Y. Advances in agronomy. 1st edition; Academic Press Inc:USA , 2014, Vol. 128: Pp 1-45.

[12]. Yulianis, Y.; Muhammad, S.; Pontas, K.; Mariana, M.; Mahidin, M. Characterization and activation of Indonesian natural zeolite from southwest aceh district-aceh province. IOP Conference Series: Materials Science and Engineering. 2018; 358: 2-7.

[13]. Omosebi, T. O.; Abass, N. F. Polymer tiles from polyethylene terephthalate (PET) wastes and fly ash: mechanical properties and durability. F1000Research. **2021**; 10:1-5.

[14]. Taiwo. O, O.; Abas, N. F. Plastic Tiles from Recycled Pet Bottles Wastes with Improved Strength and Reduced Flammability. Civil Engineering and Architecture. **2021**; 9 (5): 1-7. DOI: 10.13189/cea.2021.090508.

[15]. Fragassa, C. Limits in application of international standards to innovative ceramic solutions. International Journal for Quality Research. **2015**; 9 (2):143.

[16]. Irfan, M.; Zahid, M.; Tahir, N.; Yaseen, M.; Qazi, U.; Javaid, R.; Shahid, I. Enhanced photo-Fenton degradation of Rhodamine B using iodine-doped iron tungstate nanocomposite under sunlight. International Journal of Environmental Science and Technology. **2022**; 20: 1-16.

[17]. Sarkar, A.; Adhikary, A.; Mandal, A.; Chakraborty, T.; Das, D. Zn-BTC MOF as an adsorbent for iodine uptake and organic dye degradation. Crystal Growth & Design. **2020**; 20 (12), 7833-7839.

[18]. Anaekwe, N. O.; kailu Hassan, Y. M. Chemical Evaluation of the Glass Making Potentials of Silica Sand Deposits along Cross River in Cross River State, South–East of Nigeria. European Journal of Engineering and Technology Research. **2017**; 2 (6): 12-17.

[19]. Platias, S.; Vatalis, K. I.; Charalampides, G. Suitability of Quartz Sands for Different Industrial Applications. Procedia Economics and Finance. **2014**; 14: 491-498. DOI: 10.1016/s2212-5671(14)00738-2.

[20]. Ding, W.; Li, L.; Zhang, L.; Ju, D.; Peng, S.; Chai, W. An XPS study on the chemical bond structure at the interface between SiO_xN_y and N doped polyethylene terephthalate. The Journal of Chemical Physics. **2013**; 138 (10): 1-10.

[21]. Laurans, M.; Trinh, K.; Dalla Francesca, K.; Izzet, G.; Alves, S.; Derat, E.; Humblot, V.; Pluchery, O.; Vuillaume, D.; Lenfant, S. Covalent Grafting of Polyoxometalate Hybrids onto Flat Silicon/Silicon Oxide: Insights from POMs Layers on Oxides. ACS Applied Materials & Interfaces. **2020**; 12 (42): 28-40.

[22]. George, J.; Aaliya, B.; Sunooj, K. V.; Kumar, R. Nanotechnology-Enhanced Food Packaging. 1st edition: Wiley-VCH, New Jersey, **2022**: Pp. 235-264.

[23]. Świątczak, D.; Belica-Pacha, S.; Zawisza, A.; Kisielewska, A.; Światły-Błaszkiewicz, A.; Kupcewicz, B.; Bartosewicz, B.; Jankiewicz, B. J.; Małecka, M. Comparative study of titanium dioxide to improve the quality of finished cosmetic products. International Journal of Cosmetic Science. **2022**:1-5.

[24]. Volkov, D. S.; Rogova, O. B.; Proskurnin, M. A. Temperature dependences of IR spectra of humic substances of brown coal. Agronomy. **2021**; 11 (9): 3-10.

[25]. Jutarosaga, T.; Jeoung, J. S.; Seraphin, S. Infrared spectroscopy of Si–O bonding in low-dose low-energy separation by implanted oxygen materials. Thin Solid Films. **2018**; 476 (2): 303-311. DOI: 10.1016/j.tsf.2004.10.006.

[26]. Lin, H.; Long, J.; Gu, Q.; Zhang, W.; Ruan, R.; Li, Z.; Wang, X. In situ IR study of surface hydroxyl species of dehydrated TiO_2: towards understanding pivotal surface processes of TiO_2 photocatalytic oxidation of toluene. Physical Chemistry Chemical Physics. **2012**, 14 (26): 3-10.

[27]. Launer, P.; Arkles, B. Silicon compounds: silanes & silicones. 3rd edition; Gelest Inc, Morrisville PA 19067, **2013:** Pp. 175-178.

[28]. Soni, A.; Das, P. K.; Yusuf, M.; Kamyab, H.; Chelliapan, S. Development of sand-plastic composites as floor tiles using silica sand and recycled thermoplastics: a sustainable approach for cleaner production. Journal of Scientific reports. **2022;** 12 (1): 18921.

[29]. Awoyera, P. O.; Olalusi, O. B.; Ibia, S. Water absorption, strength and microscale properties of interlocking concrete blocks made with plastic fibre and ceramic aggregates. Case Studies in Construction Materials. **2021**;15: 2-9.

[30]. Standard, A. C373-88. Standard test method for water absorption, bulk density, apparent porosity and apparent specific gravity of fired whiteware products. ASTM International, West Conshohocken, PA. **2006:** 1-8.

[31]. Ochen, W.; D'ujanga, F. M.; Oruru, B. Effect of Quartz Particle Size on Sintering Behavior and Flexural Strength of Porcelain Tiles Made from Raw Materials in Uganda. Advances in Materials. **2019**; 8 (1): 33.

[32]. Singh, A. K.; Bedi, R.; Kaith, B. S. Composite materials based on recycled polyethylene terephthalate and their properties–A comprehensive review. Composites Part B: Engineering. **2021**; 219: 1-8.

[33]. Sahani, K.; Joshi, B. R.; Khatri, K.; Magar, A. T.; Chapagain, S.; Karmacharya, N. Mechanical Properties of Plastic Sand Brick Containing Plastic Waste. Advances in Civil Engineering. **2022**; 2022: 2-10.

[34]. Rupal, A.; Meda, S. R.; Gupta, A.; Tank, I.; Kapoor, A.; Sharma, S. K.; Sathish, T.; Murugan, P. Utilization of Polymer Composite for Development of Sustainable Construction Material. Advances in Materials Science and Engineering. **2022**; 2022: 1-10.

[35]. Lamba, P.; Kaur, D. P.; Raj, S.; Sorout, J. Recycling/reuse of plastic waste as construction material for sustainable development: A review. Environmental Science and Pollution Research. **2021;** 29(2022): 1-24.

[36]. Zanelli, C.; Soldati, R.; Conte, S.; Guarini, G.; Ismail, A. I.; El-Maghraby, M. S.; Cazzaniga, A.; Dondi, M. Technological behavior of porcelain stoneware bodies with Egyptian syenites. International Journal of Applied Ceramic Technology. **2019**; 16 (2): 574-584.

[37]. Kutanaei, S. S.; Choobbasti, A. J. Triaxial behavior of fiber-reinforced cemented sand. Journal of adhesion science and Technology. **2016**; 30 (6): 579-593.

[38]. Al-Mansour, A.; Chen, S.; Xu, C.; Peng, Y.; Wang, J.; Ruan, S.; Zeng, Q. Sustainable cement mortar with recycled plastics enabled by the matrix-aggregate compatibility improvement. Journal Construction and Building Materials. **2022**; 318:125-200.

[39]. Vahidi, G.; Bajwa, D. S.; Shojaeiarani, J.; Stark, N.; Darabi, A. Advancements in traditional and nanosized flame retardants for polymers—A review. Journal of Applied Polymer Science. **2021**; 138 (12): 1-10.

[40]. Dhawan, R.; Bisht, B. M. S.; Kumar, R.; Kumari, S.; Dhawan, S. K. Recycling of plastic waste into tiles with reduced flammability and improved tensile strength. Process Safety and Environmental Protection. **2019**; 124: 299-307. DOI: 10.1016/j.psep.2019.02.018.

[41]. Bajwa, D. S.; Rehovsky, C.; Shojaeiarani, J.; Stark, N.; Bajwa, S.; Dietenberger, M. A. Functionalized cellulose nanocrystals: A potential fire retardant for polymer composites. Polymers. **2019**; 11 (8): 1361.

[42]. Akpanyung, K.; Loto, R.; Fajobi, M. An overview of ammonium chloride (NH_4Cl) corrosion in the refining unit. Journal of Physics: Conference Series. **2019**; 1378 (2): 22-89.

[43]. Oriakhi, C. O. Chemistry in Quantitative Language: Fundamentals of General Chemistry Calculations; 2nd edition; Oxford University Press: New York, 2021: Pp. 138-425.

[44]. Benosman, A. S.; Mouli, M.; Taibi, H.; Belbachir, M.; Senhadji, Y.; Bahlouli, I.; Houivet, D. Studies on chemical resistance of PET-mortar composites: microstructure and phase composition changes. Journal of Scientific Research. **2013**; 5: 2-11.

[45]. Deka, B. K.; Mandal, M.; Maji, T. K. Effect of nanoparticles on flammability, UV resistance, biodegradability, and chemical resistance of wood polymer nanocomposite. Industrial & engineering chemistry research. **2012**; 51 (37): 1-8.

[46]. Zhang, X.; Bai, C.; Qiao, Y.; Wang, X.; Jia, D.; Li, H.; Colombo, P. Porous geopolymer composites: A review. Composites Part A: Applied Science and Manufacturing. **2021**; 150: 1-9.

[47]. Rambaldi, E.; Mazzanti, B.; Fazio, S.; Bonvicini, G.; Albertazzi, A. Chemical durability of ceramic tile surfaces in acid environment. **2012:** 2-3. https://www.qualicer.org/recopilatorio/ponencias/pdfs/2012153.pdf

[48]. Savotchenko, S.; Kovaleva, E.; Cherniakov, A. The resistance of repair epoxy composites modified with silicon-containing additives and mineral fillers. Polymer Bulletin. **2022**: 1-16.

[49]. Sang, T.; Wallis, C. J.; Hill, G.; Britovsek, G. J. Polyethylene terephthalate degradation under natural and accelerated weathering conditions. European polymer journal. **2020**; 136: 1-10

[50]. Ashassi-Sorkhabi, H.; Ghasemi, Z.; Seifzadeh, D. The inhibition effect of some amino acids towards the corrosion of aluminum in 1M HCl^+ 1M H_2SO_4 solution. Applied surface science. **2005**; 249 (1-4): 408-418.

[51]. Kühn, S.; Van Werven, B.; Van Oyen, A.; Meijboom, A.; Rebolledo, E. L. B.; Van Franeker, J. A. The use of potassium hydroxide (KOH) solution as a suitable approach to isolate plastics ingested by marine organisms. Marine Pollution Bulletin. **2017**; 115 (1-2): 86-90.

[52]. Beisch, H.; Fiedler, B. Nanocarbon Aerogels and Aerographite. Synthesis and Applications of Nanocarbons. **2020**: 247-274.

[53]. Murts, G. T.; Ram, C.; Gebru, K. A. Fabrication and characterization of cement based floor tiles using eggshell and plastic wastes as a low cost construction materials. Case Studies in Construction Materials. **2021**; 15:2-10. DOI: 10.1016/j.cscm.2021.e00747.

[54]. Tamsü, N.; Tunali, A. Parlatılmış Porselen Karoların Leke Direncini ve Temizlenebilirliğini İyileştirmek için Dolgu Malzemesinin Sol-Jel Yöntemi ile Üretilmesi Bölüm II: Proses parametrelerinin koruyucu malzemenin performansına etkilerinin incelenmesi. Afyon Kocatepe Üniversitesi Fen Ve Mühendislik Bilimleri Dergisi. **2014**; 14 (3): 141-145.